https://doi.org/10.5194/egusphere-2023-2171
Preprint. Discussion started: 28 September 2023

Extensional fault geometry and evolution within rifted margin hyper-extended continental crust leading to mantle exhumation and allochthon formation

Júlia Gómez-Romeu[1,*] & Nick Kusznir[1]

[1]*Department of Earth, Ocean and Ecological Sciences, University of Liverpool, Liverpool, UK*

[*]*Currently:* M&U sasu, *Sassenage, France*

Corresponding author: Júlia Gómez-Romeu, julia@mandu-geology.fr

Abstract

Seismic reflection interpretation at magma-poor rifted margins shows that crustal thinning within the hyper-extended domain occurs by in-sequence oceanward extensional faulting which terminates in a sub-horizontal reflector in the top-most mantle immediately beneath tilted crustal fault blocks. This sub-horizontal reflector is interpreted to be a detachment surface which develops sequentially with oceanward in-sequence crustal faulting. We investigate the geometry and evolution of active and inactive extensional faulting due to flexural isostatic rotation during magma-poor margin hyper-extension using a recursive adaptation of the rolling hinge model of Buck (1988) and compare modelling results with the seismic interpretation. In the case of progressive in-sequence faulting, we show that sub-horizontal reflectors imaged on seismic reflection data can be generated by the flexural isostatic rotation of faults with initially high-angle geometry. Flexural isostatic rotation produces shallowing of emergent fault angles, fault locking and the development of new high-angle short-cut fault segments within the hanging-wall. This results in the transfer and isostatic rotation of triangular pieces of hanging-wall onto exhumed fault footwall, forming extensional allochthons which our modelling predicts are typically limited to a few km in lateral extent and thickness. While earthquake seismology favours a planar fault geometry with in the brittle seismogenic crust, seismic reflection imaging suggests a more listric geometry. Our modelling results show that a sequence of extensional listric or planar faults with identical parameters (i.e. location, heave, surface dip, Te) produce very similar sea-bed bathymetric relief. Listric and planar fault geometries do however produce distinct Moho and allochthon shapes. We propose that the initial fault geometry, prior to flexural isostatic rotation, is planar in the seismogenic crust

https://doi.org/10.5194/egusphere-2023-2171
Preprint. Discussion started: 28 September 2023

becoming listric at depth as the brittle plastic transition is approached. Extensional faulting and thinning of hyper-extended continental crust may eventually lead to mantle exhumation. Where extensional faulting is in-sequence, this results in a smooth bathymetric transition from thinned continental crust to exhumed mantle. In contrast out-of- sequence faulting results in a transition to exhumed mantle with bathymetric relief.

1. Introduction

The hyper-extended domain of magma-poor rifted margins is formed when continental crust is thinned to approximately 10 km or less and the crust becomes fully brittle allowing faults to penetrate through the entire crust into the mantle (Pérez-Gussinyé et al., 2001; Manatschal, 2004; Tugend et al. 2014). It has a crustal architecture characterised by oceanward tilting crustal fault blocks often underlain by a strong coherent sub-horizontal seismic reflector (Krawczyk et al., 1996; Reston et al., 1996).

The geometry and evolution of extensional faults within the hyper-extended domain has been a long-standing question. Interpretation of past and recently acquired high-quality seismic reflection images (Ranero and Pérez-Gussinyé, 2010; Lymer et al., 2019) has revealed that crustal thinning within the hyper-extended domain occurs by oceanward in-sequence extensional faults (Figure 1). These faults are shown to detach into the sub-horizontal seismic reflector beneath the crustal fault block which is interpreted to be a sub-horizontal detachment within the top-most mantle. This detachment has been shown to develop sequentially as extensional crustal faulting above propagates oceanward in-sequence to form the observed continuous structure as imaged on seismic data (Lymer et al., 2019).

In this paper we investigate the geometry and evolution of extensional faults within the hyper-extending brittle crust of a magma-poor margin using a numerical model which determines the flexural isostatic response to crustal thinning by sequential faulting. Using this model, which is an adaptation of the rolling hinge model of Buck (1988), we examine how both active and inactive fault geometries are modified during sequential faulting by flexural isostatic rotation to form the sub-horizonal structure imaged on seismic reflection data. In addition we examine the transition from hyper-extended continental crust to exhumed mantle and how it depends on the sequence of extensional faulting.

A long-standing question is whether the initial geometry of crustal extension faults is planar or listric; earthquake seismology and geodetic observations favour a planar geometry (Jackson

https://doi.org/10.5194/egusphere-2023-2171
Preprint. Discussion started: 28 September 2023

1987; Stein & Barrientos 1985) while seismic reflections imaging suggests a more listric geometry. Using the flexural isostatic rotation model, we also investigate whether an initial listric or planar fault geometry better fits seismic observations of the sub-horizontal reflector and the geometry of extensional allochthons.

2. Model formulation

We use a numerical model (RIFTER) to replicate faulting and fault block geometry within the hyper-extended domain, and to investigate fault rotation, fault geometry interaction, the formation of crustal allochthon blocks and the transition between hyper-extended and exhumed mantle domains. RIFTER is a kinematic forward lithosphere deformation model that allows the production of flexural isostatically compensated as well as balanced cross-sections. Within RIFTER, lithosphere is deformed by faulting in the upper crust with underlying distributed pure-shear deformation in the lower crust and mantle. A key attribute of RIFTER is that it incorporates the flexural isostatic response to extensional faulting and crustal thinning. Therefore, RIFTER can be used to model and predict the structural development of extensional tectonic settings (Figure 2). The model is kinematically controlled with fault geometry and displacement and pure-shear distribution given as model inputs as a function of time. Lithosphere flexural strength, parameterised as lithosphere effective elastic thickness, is also defined. Model outputs are geological cross-sections which are flexural isostatically compensated as well as structurally balanced (Figure 2). The kinematic formulation of RIFTER represents an advantage over dynamic modelling because the input data given to RIFTER can be constrained by observed geology. In addition, RIFTER provides for the isostatic testing of palinspastic cross-sections and can also be used to explore different kinematic scenarios. A more detailed description of the model formulation (originally called OROGENY) is given by Toth et al., (1996), Ford et al., (1999) and Jácome et al., (2003). These studies show the model formulation applied to compressional tectonics however similar physical principles apply for an extensional tectonics scenario. Gómez-Romeu et al., (2019) show how RIFTER can be used to reproduce both extensional and compressional tectonics using the Western Pyrenees as a case-study.

Within RIFTER, loads resulting from extensional lithosphere deformation are assumed to be compensated by flexural isostasy. The lithosphere flexural strength must be considered to determine the isostatic rotation of faults during extension and therefore to investigate their geometric evolution. These loads are generated by faulting, crustal thinning, sedimentation,

https://doi.org/10.5194/egusphere-2023-2171
Preprint. Discussion started: 28 September 2023

erosion and lithosphere thermal perturbation and re-equilibration (Kusznir et al., 1991). For the purposes of calculating the flexural isostatic response, the lithosphere is represented as an elastic plate of effective elastic thickness (Te) floating on a fluid substratum. The lithosphere effective elastic thickness (Te) is defined as the equivalent thickness of a perfectly elastic plate which has the same flexural strength as the lithosphere. Extension on basement faults produces flexure which, as well as generating footwall uplift and hangingwall subsidence, gives rise to substantial bending stresses (Magnavita et al., 1994) in the cooler upper lithosphere; these large bending stresses are reduced by combined brittle and plastic failure. The flexural strength of the lithosphere, and therefore Te, are reduced by this brittle and plastic failure and this reduction becomes greater with increase in extension (Magnavita et al., 1994). Therefore, in extensional tectonic settings, a low effective elastic thickness (Te) is expected and required to reproduce the consequences of lithosphere deformation due to extensional faulting.

We use a Te value of 0.5 km associated to each fault for the development of the transition between the hyper-extended domain and the initiation of exhumed mantle domain (Figure 3). This value is consistent with those determined at slow-spreading ocean ridges ranging between 0.5 and 1 km (e.g. Smith et al., 2008; Schouten et al., 2010; Buck, 1988) where a similar lithosphere flexural strength to that of the distal rifted margins is expected.

The initial crustal geometry for our modelling of extensional faulting within the hyper-extended domain leading to mantle exhumation and allochthon formation is when the continental crust has been thinned down to 10 km (Tugend et al., 2014) corresponding to the point when faults within the seismogenic layer couple into the mantle (Pérez-Gussinyé et al., 2001). Prior to that, during the necking zone stage of margin formation (Mohn et al., 2012), faults are expected to be decoupled from the mantle by ductile deformation within the lower continental crust. The width of the necking zone with crust 10 km thick at the start of hyper-extension is set to 100 km although this width value is not critical to this study. The starting bathymetry is set to 2 km corresponding to the isostatic equilibrium of continental crust thinned to 10 km with an highly elevated lithosphere geotherm (Figure 3b). For simplicity we only model faulting during hyper-extension on one distal rifted margin and do not include faulting within its distal conjugate. This simplified initial model template allows us to focus on extensional faulting during the formation of a distal magma-poor rifted margin avoiding the complexity occurring during the earlier rifting and necking phases. Figure 3c shows the resultant model of a distal rifted margin formation. The detailed numerical model stages to produce this are shown in Figures 3d-e and described below for the formation of the hyper-

https://doi.org/10.5194/egusphere-2023-2171
Preprint. Discussion started: 28 September 2023

extended domain, the initiation of the exhumed mantle domain and the formation of extensional allochthons.

3. Model application to sequential faulting within the hyper-extended margin domain

The interpretation of sub-horizontal seismic reflectors below fault blocks within the hyper-extended domain has been intensively debated (e.g. Reston et al., 1996). Interpretations suggested for these structures (H and S type-reflectors in Galicia margin and Iberia Abyssal Plain respectively, de Charpal et al., 1978; Krawczyk et al., 1996) are multiple and reviewed later in the discussion. Despite this wide range of possible interpretations, after the work by Reston et al. (1996) and Krawczyk et al. (1996), it has been generally accepted that the H and S reflectors are detachment faults (Manatschal et al., 2001). Ranero & Pérez-Gussinyé (2010) suggested that extensional faulting within the hyper-extended domain develops oceanward in-sequence with initially steeply dipping faults. As in-sequence faulting propagates oceanward, active fault rotation modifies the deeper geometry of previously active faults leading to their deeper segments being passively rotated to a lower angle producing an apparent listric fault geometry or even a sub-horizontal appearance. Lymer et al., (2019) confirmed observationally that extensional faulting develops oceanward in-sequence, and that extensional faulting soles out into the sub-horizontal detachment imaged as the H and S type-reflectors.

Figure 3d shows the modelling results of progressive deformation within the hyper-extended domain resulting from a set of in-sequence extensional faults. The initial pre-movement dip of each extensional fault at the surface is 60^{o}. In the model results shown in Figure 3d-e the faults detach at 15 km depth corresponding to an assumed brittle-plastic transition within the top-most mantle (results obtained from an initial planar fault geometry are examined later). Flexural isostatic response to faulting leads to an uplift of the footwall block, subsidence of the hanging-wall block and a rotation of the active fault plane reducing its dip (Figure 3d1). The reduction of fault dip due to flexural isostatic rotation is expected to lead to the locking of that fault and the initiation of new faults with steeper dip. This is shown in Figure 3d2 and subsequent Figures 3d3-6.

Extension on each new fault not only reduces its own fault dip by flexural isostatic rotation but also further reduces the fault dip of earlier active faults within its footwall. The cumulative result of this process is that faults originally steeply dipping when active become sub-horizontal

https://doi.org/10.5194/egusphere-2023-2171
Preprint. Discussion started: 28 September 2023

in their lower parts as illustrated in Figures 3d5 for fault number 1. In this case the sub-horizontal inactive fault is almost coincident with the Moho beneath the hyper-extended continental crustal fault-blocks (Figure 3d5). If fault extension is sufficiently large and the hyper-extended continental crust is sufficiently thin, footwall exhumation leads to mantle exhumation (Figure 3d6) (Manatschal et al., 2001).

Table 1 summarizes the fault parameters and sequential fault displacement required to reproduce the structural architecture of the hyper-extended domain shown in Figure 3d.

4. Model application to mantle exhumation and extensional allochthon formation

For even greater extension on the exhumation fault, the exhumed mantle footwall becomes sub-horizontal at the sea-bed due to flexural isostatic rotation as predicted by the rolling-hinge model of Buck (1988). Extensional allochthon blocks sitting above sub-horizontal exhumed footwall are observed at magma-poor margins by seismic reflection imaging and field studies (Epin and Manatschal and references therein, 2018).

We use RIFTER to investigate the formation of extensional allochthon blocks by the rolling-hinge model as suggested by Manatschal et al., (2001) and shown in Figure 3e. Allochthon blocks are produced by new steeply dipping extensional faults cutting through the hangingwall block of a master fault (fault 6 in our case in Figure 3e1) and pulling off triangular pieces of continental crust from the hanging-wall (i.e. the rolling hinge model of Buck, 1988). These new faults, created when the emergence angle of the master fault becomes too low (~30° dip), are short-cuts of the master fault and connect with it at depth. Depending on what depth they initiate at and their break-away position, the size of the crustal allochthon block generated will vary (Figure 3e). The intersection depth between the master fault and the new extensional faults is different in each model stage shown in Figure 3e but it ranges between 5 and 10 km depth consistent with deMartin et al., (2007). Another parameter that differs in each model stage is the distance between two consecutive allochthon blocks. This depends on how much the new extensional fault moved before it locked. A small fault offset will not generate exhumed mantle between two allochthon blocks as shown in Figures 3e3-4 whereas a large fault offset will generate exhumed mantle and a sub-horizontal sea-bed geometry between two allochthon blocks (Figures 3e4-5). Note that each allochthon block overlies sub-horizontal exhumed footwall generated by flexural isostatic rotation.

https://doi.org/10.5194/egusphere-2023-2171
Preprint. Discussion started: 28 September 2023

Table 2 summarizes the initial fault parameters and the chronological fault displacement required to reproduce the structural architecture of the exhumed mantle domain shown in Figure 3e.

5. Sensitivity to listric or planar fault geometry?

Lithosphere deformation is achieved by localised deformation on faults and shear zones within the upper lithosphere with distributed deformation below at depth. A long-standing question is how deformation by faulting connects to deep distributed lithosphere deformation. This question also has implications for fault geometry. Our numerical experiments described above in sections 3 and 4 assume a listric fault geometry in which faults sole out into a sub-horizontal shear zone at 15 km depth below which deformation becomes distributed. In contrast earthquake seismology and geodetic analysis (Stein and Barrientos, 1985; Jackson, 1987) suggests that large extensional earthquakes involve faults whose geometry is planar above an interpreted brittle-ductile transition.

We explore the differences between using listric and planar fault in modelling the formation of the hyper-extended and exhumed mantle domains. The results are compared in Figure 4. The initial faults geometries for listric and planar faults are shown in Figures 4a and d respectively. Both have an initial surface dip of 60°. The initial listric fault geometry soles out at 15 km while the initial planar fault geometry continues downwards with a dip of 60°. We assume that the deformation transition from faulting to distributed deformation for the planar fault occurs within the mantle below the crust-mantle density interface and so does not affect the isostatic response to faulting.

Listric and planar fault geometry model predictions are shown in Figures 4c and f and use the same fault locations, fault extension and sequence. Comparison shows that listric and planar fault geometries produces very similar sea-bed structural topography, and which cannot be used to distinguish whether fault geometry is listric or planar. In contrast, the listric and planar fault models produce different sub-surface structure. The Moho geometries predicted by the listric and planar fault geometry models are also different, however whether these different predicted Moho geometries can be distinguished using seismic reflection data is uncertain.

In section 4 we used listric fault geometries to model allochthon formation. We now examine allochthon formation using planar faults and compare these predictions with those using listric faults (Figure 5). For both listric and planar fault geometries, Figure 5 shows the formation of

https://doi.org/10.5194/egusphere-2023-2171
Preprint. Discussion started: 28 September 2023

allochthons for different separations of the hanging-wall short-cut fault from the primary extensional fault which has exhumed mantle footwall. Separations of 1 km (Figures 5a-b and g-h), 2 km (Figures 5c-d and i-j) and 5 km (Figures 5 e-f and k-l) are used. For the 1 km separation, a small allochton is produced with similar triangular geometry for both listric (Figure 5b) and planar (Figure 5h) fault geometries. Increasing the separation to 2 km increases the allochthon size; however while the listric fault (Figure 5d) produces a triangular allochthon, the planar fault (Figure 5j) geometry produces a 4-sided body. For a 5 km separation, the allochthon size increases further and both listric (Figure 5f) and planar (Figure 5l) fault geometries produce a 4- sided body. For the larger separations of the short-cut fault from the primary fault, the detached fragment transferred to the exhumed mantle consists of continental basement with some autochthonous mantle beneath it (Figure 5j-l). Whether extensional allochthons can provide insight into answering the question whether extensional faults are listric or planar poses an interesting challenge.

6. The transition from hyper-extended crust to exhumed mantle and its sensitivity to in-sequence vs out-of-sequence faulting

Stretching and thinning of the continental crust can eventually lead to mantle exhumation as observed by drilling on the distal Iberian margin (Figures 6a-b). Seismic reflection data (Figure 6c) provides insight into how mantle exhumation was achieved by extensional faulting. Based on drill and seismic reflection data, Manatschal et al., (2001, 2004) proposed that an in-sequence ocean-ward propagating set of extensional faulting progressively thins the continental crust in the hyper-extended domain until eventually a large extensional fault exhumes mantle in its footwall. Our modelling of mantle exhumation using a set of in-sequence extensional faults as proposed by Manatschal et al., (2001, 2004) is shown in Figure 3 and 7a. and produces a smooth bathymetric transition from continental crust to exhumed mantle.

While the in-sequence fault extension process provides a very good generalised model for the formation of the hyper-extended margin domain, mantle exhumation and their transition, it is unlikely that all faults propagate in-sequence oceanward. Some out-of-sequence faulting is to be expected when the 3D nature and along strike complexity of rifting and breakup is considered and can be seen seismically in Figure 6e. In Figure 7b we show the result of introducing an out-of-sequence fault, with the same dip sense as other faults, into the hyper-extension and mantle exhumation model. All other faults have similar locations and extensions to those used to produce Figure 7a. The effect of introducing an out-of-sequence fault to

https://doi.org/10.5194/egusphere-2023-2171
Preprint. Discussion started: 28 September 2023

exhume mantle is to produce a transition from thinned continental crust to mantle which is no longer smooth at the seabed but shows bathymetric relief. An out-of-sequence fault might also have an opposite dip-sense as shown in Figure 7c. This fault does not exhume mantle but does generate a horst containing exhumed mantle capped by thinned continental crust as observed in Figure 6e.

7. Discussion

To better understand extensional fault geometry and its evolution during hyper-extension at magma-poor rifted margins, several important questions need to be answered: (i) are faults active at low angle, (ii) what is the sub-horizontal reflector, (iii) do extensional faults have a listric or planar geometry and (iv) is faulting in-sequence or out-of-sequence.

In section 4 (Figure 3) we show for a listric fault geometry that flexural isostatic rotation progressively reduces the fault dip of inactive faults within the footwall of oceanward in-sequence faulting. From this we can deduce that the present day sub-horizontal orientation of a fault at depth does not indicate that the fault was active at a sub-horizontal orientation. This conclusion is consistent with the modelling results of Ranero & Pérez-Gussinyé, (2010) and the interpretations of seismic observations of Lymer et al. (2019).

The nature of the seismically imaged sub-horizontal reflectors beneath rotated fault blocks in the hyper-extended domain has been extensively debated (e.g. Reston et al. 1996; Lymer et al. 2019 and references therein). Proposed origins of the sub-horizontal reflector have included a lithosphere scale extensional detachment fault (Wernicke et al., 1981), the top of a mafic underplate (Horsefield, 1992), a thin igneous intrusion (Reston, 1996), a serpentinization front (Boillot et al., 1987), and the brittle-plastic transition (de Charpal et al., 1978; Sibuet, 1992). Detailed seismology by Reston et al., (1996) was able to eliminate an igneous origin, leaving the brittle-plastic transition in the top-most mantle as the most likely interpretation, probably assisted by mantle serpentinization. Seismic reflection interpretation shows that extensional faults thinning the continental crust within the hyper-extended domain sole out into the sub-horizontal reflector which is located either at the base of the thinned continental crust or slightly deeper within the top-most mantle (Reston et al. 1996; Manatschal et al., 2001). If extensional faults within the hyper-extended zone penetrate into the mantle, as suggested by Pérez-Gussinyé et al., (2001), then the interpretation of seismically observed sub-horizontal reflectors

https://doi.org/10.5194/egusphere-2023-2171
Preprint. Discussion started: 28 September 2023

being the brittle-plastic transition requires that transition to be within the mantle rather than at the base of the thinned continental crust.

Analysis of the recently acquired 3D seismic reflection data in the hyper-extended southern Galicia margin by Lymer et al. (2019) shows that oceanward in-sequence extensional crustal faulting detaches into a sub-horizontal detachment imaged as the sub-horizontal reflector (confirming the interpretations of Manatschal et al.; 2001 and Ranero & Pérez-Gussinyé: 2010) and that the sub-horizontal detachment develops oceanward synchronously with the in-sequence crustal faulting.

Our listric fault model (Figure 4a-c) assumes that faults sole out into a horizontal detachment within the mantle at 15 km depth consistent with the seismically observed sub-horizontal reflectors being interpreted as the transition from localised brittle deformation above to distributed plastic deformation below. Our model predictions are also consistent with the interpretation of Lymer et al., (2019) that the sub-horizontal reflector is the relict of an ocean-ward propagating detachment at the base of the in-sequence crustal faulting and is not simultaneously active from distal to proximal.

In section 5 (Figure 4) we compare the response of listric and planar fault geometries for oceanward in-sequence hyper-extension. Significant flexural isostatic rotation leading to greatly reduced dip of planar faults at depth is also seen, especially for planar faults in the footwall of later faults with large extension. However, Figure 4 shows a clear difference between planar (Figures 4d-f) and listric (Figures 4a-c) fault geometries at depth; planar fault geometries do not result in a continuous sub-horizontal structure at depth. In contrast because all listric faults sole out at the same brittle-plastic transition depth, all listric faults form a single continuous sub-horizontal structure at depth resembling that observed on seismic reflection data in the hyper-extended domain. The fault geometries at depth generated by listric faulting appear to be similar to structures seismically imaged at depth.

Earthquake seismology, however, favours a planar fault geometry for extension within the seismogenic layer (Stein and Barrientos, 1985; Jackson, 1987). How might extensional deformation on a planar fault in the brittle seismogenic layer evolve into distributed plastic deformation at depth? In the case of rifted margin hyper-extension, extensional faults may permit water to penetrate down into the top-most mantle (e.g. Pérez-Gussinyé et al., 2001) enabling mantle serpentinization to occur. If this occurs, serpentinized upper mantle at the base of extensional faults would provide a weak layer enabling the formation of a horizontal

https://doi.org/10.5194/egusphere-2023-2171
Preprint. Discussion started: 28 September 2023

detachment (Lymer et al. 2019 and references therein). Planar faulting in the seismogenic layer might then sole out into this horizontal detachment in the top-most mantle immediately beneath thinned continental crust. The resulting fault geometry would not be dissimilar to that of the listric fault used in the modelling of sections 3 and 4 but with a more planar geometry in the upper brittle seismogenic layer.

The rolling hinge model of Buck (1988) provides an explanation for the formation of triangular allochthons of continental crust emplaced on exhumed mantle (Buck 1988; Manatchal et al. 2001; Epin & Manatschal, 2019). In Figures 3 and 5 we show slivers of hanging wall continental crust transferred onto exhumed mantle footwall by short-cut faults. Flexural isostatic rotation produces the observed geometry of triangular allochthons emplaced on sub-horizontal exhumed mantle. While listric and planar fault geometries produce nearly identical small allochthons, their difference becomes pronounced for large allochthons (Figure 5). Listric faults always produce a triangular allochthon fragment of hanging-wall continental crust while planar faults produce a rectangular shape for large allochthons (semantically these large rectangular fragments produced by planar faults should perhaps be called autochthons). Whether reflection seismology observations of large allochthon shapes can be used to distinguish listric or planar fault geometry during hyper-extension remains to be investigated.

Oceanward in-sequence faulting shown in Figure 3 and as proposed by Manatschal et al. (2001) and Manatschal (2004) provides a good generalised model for the formation of hyper-extended magma-poor margins. However, it should be recognised that out-of-sequence faulting does occur during margin formation and is the inevitable consequence of the 3D nature of continental breakup at the regional scale where upper-plate/lower-plate polarity varies along margin strike. Lymer et al., (2019) also show that, at the more local scale, 3D fault system overlap must occur and would also break a simple oceanward in-sequence fault pattern. The transition from hyper-extended continental crust to exhumed mantle is particularly sensitive to the sequence of faulting; oceanward in-sequence faulting produces a smooth bathymetric transition onto exhumed mantle while out of sequence produces a transition with bathymetric relief as shown in Figure 7.

https://doi.org/10.5194/egusphere-2023-2171
Preprint. Discussion started: 28 September 2023

8. Summary

a) Flexural isostatic rotation of extensional faulting (the rolling hinge model) applied to the formation of the hyper-extended domain of magma-poor rifted margins predicts fault geometry evolution consistent with the interpretations of seismic reflection data.

b) The same modelling shows that seismically observed low-angle extensional faults were not necessarily active at low angle and have been flexurally rotated to their present low angle geometry.

c) The observed geometry of extensional allochthons are consistent with extensional faults soling out into a horizontal detachment in the topmost mantle probably controlled by mantle serpentinization. Extensional faults may initially have a planar geometry in the upper seismogenic layer but this initial planar geometry is modified by flexural isostatic rotation.

d) Sequential in-sequence oceanward extensional faulting is the dominant process during the extensional thinning of the hyper-extended domain at magma-poor rifted margins. Some out-of-sequence faulting does occur and generates a recognisably distinct transition onto exhumed mantle.

Author contribution

JGR: Conceptualization, Formal analysis, Investigation, Methodology, Visualization, Writing – original draft preparation, Writing – review and editing. **NK**: Conceptualization, Formal analysis, Funding acquisition, Investigation, Methodology, Project administration, Software, Supervision, Visualization, Writing – review and editing.

Competing interests

The authors declare that they have no conflict of interest.

Acknowledgments

We acknowledge the MM4 (Margin Modelling Phase 4) industry partners (BP, Conoco Phillips, Statoil, Petrobras, Total, Shell, BHP-Billiton, and BG) for financial support and discussions.

References

Beslier, M.O., Ask, M., Boillot, G., 1993. Ocean-continent boundary in the Iberia Abyssal Plain from multichannel seismic data. Tectonophysics 218, 383–393. https://doi.org/10.1016/0040-1951(93)90327.

Boillot, G., Recq, M., Winterer, E.L., Meyer, A.W., Applegate, J., Baltuck, M., Bergen, J.A., Comas, M.C., Davies, T.A., Dunham, K., Evans, C.A., Girardeau, J., Goldberg, G., Haggerty, J., Jansa, L.F., Johnson, J.A., Kasahara, J., Loreau, J.P., Luna-Sierra, E., Moullade, M., Ogg, J., Sarti, M., Thurow, J., Williamson, M., 1987. Tectonic denudation of the upper mantle along passive margins: a model based on drilling results (ODP leg 103, western Galicia margin, Spain). Tectonophysics 132, 335–342. https://doi.org/10.1016/0040-1951(87)90352-0.

Buck, W.R., 1988. Flexural Rotation of Normal Faults. Tectonics 7, 959–973.

De Charpal, O., Guennoc, P., Montadert, L., Roberts, D.G., 1978. Rifting, crustal attenuation and subsidence in the Bay of Biscay. Nature 275, 706–711. https://doi.org/10.1038/275706a0.

deMartin, B.J., Sohn, R.A., Canales, J.P., Humphris, S.E., 2007. Kinematics and geometry of active detachment faulting beneath the Trans-Atlantic geotraverse (TAG) hydrothermal field on the Mid-Atlantic Ridge. Geology 35, 711–714. https://doi.org/10.1130/G23718A.1.

Epin, M. E., & Manatschal, G. (2018). Three-dimensional architecture, structural evolution, and role of inheritance controlling detachment faulting at a hyper-extended distal margin: The example of the Err detachment system (SE Switzerland). Tectonics, 37(12), 4494-4514.

Ford, M., Lickorish, W.H., Kusznir, N.J., 1999. Tertiary foreland sedimentation in the Southern Subalpine Chains, SE France: A geodynamic appraisal. Basin Res. 11, 315–336. doi:10.1046/j.1365-2117.1999.00103.x.

Gómez-Romeu, J., Masini, E., Tugend, J., Ducoux, M., & Kusznir, N. (2019). Role of rift structural inheritance in orogeny highlighted by the Western Pyrenees case-study. Tectonophysics, 766, 131-150.

https://doi.org/10.5194/egusphere-2023-2171
Preprint. Discussion started: 28 September 2023

Hoffmann, H.J., Reston, T.J., 1992. Nature of the S reflector beneath the Galicia Banks rifted margin: preliminary results from prestack depth migration. Geology 20, 1091–1094. https://doi.org/10.1130/0091-7613(1992)020<1091:NOTSRB>2.3.CO;2.

Horsefield, S.J., 1992. Crustal structure across the contiennt-ocean boundary [Ph.D. thesis]. Cambridge Univ.

Jackson, J. a., 1987. Active normal faulting and crustal extension. Geol. Soc. London, Spec. Publ. 28, 3–17. https://doi.org/10.1144/GSL.SP.1987.028.01.02.

Jácome, M.I., Kusznir, N., Audemard, F., Flint, S., 2003. Formation of the Maturín Foreland Basin, eastern Venezuela: Thrust sheet loading or subduction dynamic topography. Tectonics 22, n/a-n/a. https://doi.org/10.1029/2002tc001381.

Krawczyk, C.M., Reston, T.J., Beslier, M.O., Boillot, G., 1996. Evidence for Detachment Tectonics on the Iberia Abyssal Plain Rifted Margin 149, 1–13. https://doi.org/10.2973/odp.proc.sr.149.244.1996.

Kusznir, N.J., Marsden, G., Egan, S.S., 1991. A flexural-cantilever simple-shear/pure-shear model of continental lithosphere extension: applications to the Jeanne d'Arc Basin, Grand Banks and Viking Graben, North Sea. Geol. Soc. London, Spec. Publ. 56, 41–60. https://doi.org/10.1144/gsl.sp.1991.056.01.04.

Lymer, G., Cresswell, D.J.F., Reston, T.J., Bull, J.M., Sawyer, D.S., Morgan, J.K., Stevenson, C., Causer, A., Minshull, T.A., Shillington, D.J., 2019. 3D development of detachment faulting during continental breakup. Earth Planet. Sci. Lett. 515, 90–99. https://doi.org/10.1016/j.epsl.2019.03.018.

Magnavita, L.P., Davison, I., Kusznir, N.J., 1994. Rifting, erosion, and uplift history of the Reconcavo-Tucano-Jatoba Rift, northeast Brazil. Tectonics 13, 367–388.

Manatschal, G., 2004. New models for evolution of magma-poor rifted margins based on a review of data and concepts from West Iberia and the Alps. Int. J. Earth Sci. 93, 432–466. https://doi.org/10.1007/s00531-004-0394-7.

Manatschal, G., Froitzheim, N., Rubenach, M., Turrin, B.., 2001. The role of detachment faulting in the formation of an ocean-continent transition: insights from the Iberia Abyssal Plain from: Wilson, R.C.L., Whitmarsh, R.B., Taylor, B. & Froitzheim, N. Non-Volcaninc Rifting of Continental Margins: A Comparison of Evid. Geol. Soc. London, Spec. Publ.

187, 405–428. https://doi.org/0305-8719/01/1500.

Mohn, G., Manatschal, G., Beltrando, M., Masini, E., & Kusznir, N. (2012). Necking of continental crust in magma-poor rifted margins: Evidence from the fossil Alpine Tethys margins. Tectonics, 31(1).

Montadert, L., De Charpal, O., Roberts, D., Guennoc, P., Sibuet, J.-C., 1979. Northeast Atlantic passive continental margins: Rifting and subsidence processes. In: Talwani, M., Hay, W. & Ryan, W. B. F. (eds) Deep Drilling Results in the Atlantic Ocean: Continental Margins and Palaeoenvironments. Am. Geophiscal Union, Washington, DC 154–186.

Pérez-Gussinyé, M., 2013. A tectonic model for hyperextension at magma-poor rifted margins: an example from the West Iberia – Newfoundland conjugate margins. Geol. Soc. London, Spec. Publ. 369, 403–427. https://doi.org/10.1144/SP369.19.

Pérez-Gussinyé, M., Reston, T.J., Morgan, J.., 2001. Serpentinization and magmatism during extension at non-volcanic margins: the effect of initial lithospheric structure. Geol. Soc. London, Spec. Publ. 187, 551–576. https://doi.org/10.1144/GSL.SP.2001.187.01.27.

Péron-Pinvidic, G., Manatschal, G., Minshull, T.A., Sawyer, D.S., 2007. Tectonosedimentary evolution of the deep Iberia-Newfoundland margins: Evidence for a complex breakup history. Tectonics 26, 1–19. https://doi.org/10.1029/2006TC001970.

Péron-Pinvidic, G., Manatschal, G., Osmundsen, P.T., 2013. Structural comparison of archetypal Atlantic rifted margins: A review of observations and concepts. Mar. Pet. Geol. 43, 21–47. https://doi.org/10.1016/j.marpetgeo.2013.02.002.

Ranero, C.R., Pérez-Gussinyé, M., 2010. Sequential faulting explains the asymmetry and extension discrepancy of conjugate margins. Nature 468, 294–299. https://doi.org/10.1038/nature09520.

Reston, T.J., 2005. Polyphase faulting during the development of the west Galicia rifted margin. Earth Planet. Sci. Lett. 237, 561–576. https://doi.org/10.1016/j.epsl.2005.06.019.

Reston, T.J., 1996. The S reflector west of Galicia: The seismic signature of a detachment fault. Geophys. J. Int. 127, 230–244. https://doi.org/10.1111/j.1365-246X.1996.tb01547.

Reston, T.J., Krawczyk, C.M., Klaeschen, D., 1996. The S reflector west of Galicia (Spain): Evidence from prestack depth migration for detachment faulting during continental breakup. J. Geophys. Res. Solid Earth 101, 8075–8091.

https://doi.org/10.5194/egusphere-2023-2171
Preprint. Discussion started: 28 September 2023

https://doi.org/10.1029/95jb03466.

Reston, T.J., McDermott, K.G., 2011. Successive detachment faults and mantle unroofing at magma-poor rifted margins. Geology 39, 1071–1074. https://doi.org/10.1130/G32428.1.

Roberts, A.M., Kusznir, N.J., Yielding, G., Beeley, H., 2019. Mapping the bathymetric evolution of the northern North Sea: from Jurassic syn-rift archipelago through Cretaceous-Tertiary post-rift subsidence. Pet. Geosci.

Roberts, A.M., Kusznir, N.J., Yielding, G., Styles, P., 1998. 2D flexural backstripping of extensional basin: the need for a sideways glance. Pet. Geosci. 4, 327–338. https://doi.org/10.1144/petgeo.4.4.327.

Schouten, H., Smith, D.K., Cann, J.R., Escartín, J., 2010. Tectonic versus magmatic extension in the presence of core complexes at slow-spreading ridges from a visualization of faulted seafloor topography. Geology 38, 615–618. https://doi.org/10.1130/G30803.1.

Sibuet, J.-C., 1992. Formation of non-volcanic passive margins: a composite model applies to the conjugate Galicia and southeastern Flemish cap margins. Geophys. Res. Lett. 19, 769–772.

Smith, D.K., Escartín, J., Schouten, H., Cann, J.R., 2008. Fault rotation and core complex formation: Significant processes in seafloor formation at slow-spreading mid-ocean ridges (Mid-Atlantic Ridge, 13°-15°N). Geochemistry, Geophys. Geosystems 9. https://doi.org/10.1029/2007GC001699.

Stein, R.-S., Barrientos, S.-E., 1985. Planar High-Angle Faulting in the Basin and Range: Geodetic Analysis of the 1983 Borah Peak, Idaho, Earthquake. J. Geophys. Res. 90, 11,355-11,366.

Sutra, E., Manatschal, G., 2012. How does the continental crust thin in a hyper-extended rifted margin? Insights from the iberia margin. Geology 40, 139–142. https://doi.org/10.1130/G32786.1.

Sutra, E., Manatschal, G., Mohn, G., Unternehr, P., 2013. Quantification and restoration of extensional deformation along the Western Iberia and Newfoundland rifted margins. Geochemistry, Geophys. Geosystems 14, 2575–2597.

Toth, J., Kusznir, N.J., Flint, S.S., 1996. A flexural isostatic model of lithosphere shortening and foreland basin formation: Application to the Eastern Cordillera and Subandean belt of NW Argentina. Tectonics 15, 2–3.

Tugend, J., Manatschal, G., Kusznir, N.J., Masini, E., Mohn, G., Thinon, I., 2014. Formation and deformation of hyper-extended rift systems: Insights from rift domain mapping in the Bay of Biscay-Pyrenees. Tectonics 33, 1239–1276.

Wernicke, B., 1981. Low-angle normal faults in the Basin and Range Province: nappe tectonics in an extending orogen. Nature 291, 645–648. https://doi.org/10.1038/291645a0.

White, R.S., 1999. The lithosphere under stress. Philos. Trans. R. Soc. A Math. Phys. Eng. Sci. 357, 901–915. https://doi.org/10.1098/rsta.1999.0357.

Whitmarsh, R.B., Manatschal, G., Minshull, T. a, 2001. Evolution of magma-poor continental margins from rifting to seafloor spreading. Nature 413, 150–154. https://doi.org/10.1038/35093085.

Whitmarsh, R.B., Pinheiro, L.M., Miles, P.R., Recq, M., Sibuet, J.-C., 1993. Thin crust at the western Iberia ocean-continent transition and ophiolites. Tectonics 12, 5.

https://doi.org/10.5194/egusphere-2023-2171
Preprint. Discussion started: 28 September 2023

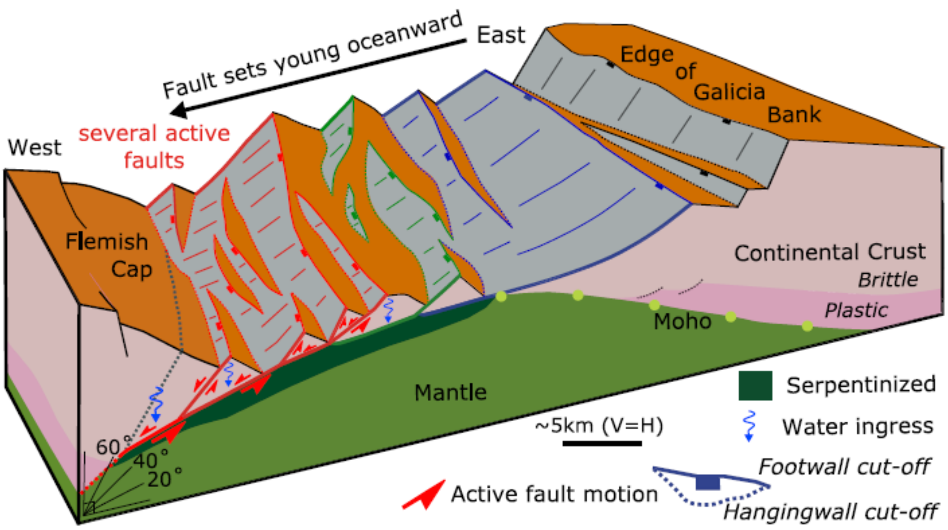

Figure 1: Summary model of extensional faulting within the hyper-extended domain of the Iberia magma-poor rifted margin based on 3D seismic reflection interpretation (Lymer et al. 2019).

https://doi.org/10.5194/egusphere-2023-2171
Preprint. Discussion started: 28 September 2023

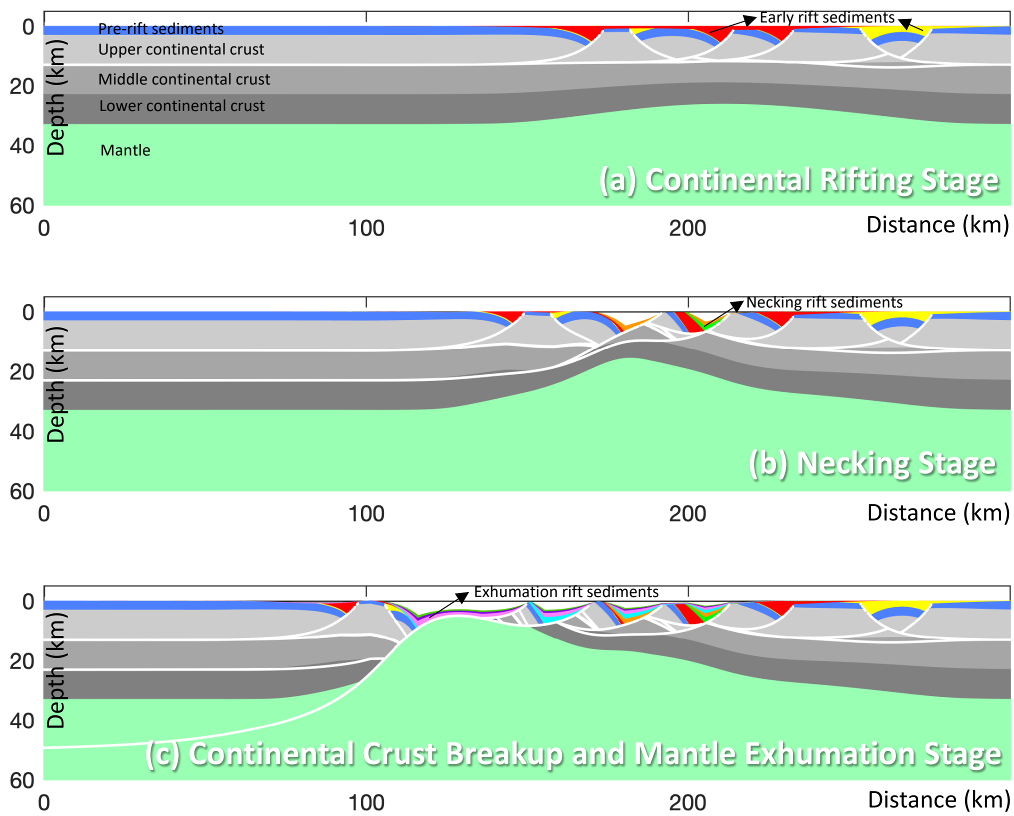

Figure 2: Example application of the kinematic lithosphere deformation model (RIFTER) applied to magma-poor rifted margin development: **a) c**ontinental rifting stage, **b) n**ecking stage, **c)** crustal breakup and mantle exhumation stage. The model computes the flexural isostatic response to changes in lithosphere loading including the rolling hinge flexural rotation process during extensional faulting.

https://doi.org/10.5194/egusphere-2023-2171
Preprint. Discussion started: 28 September 2023

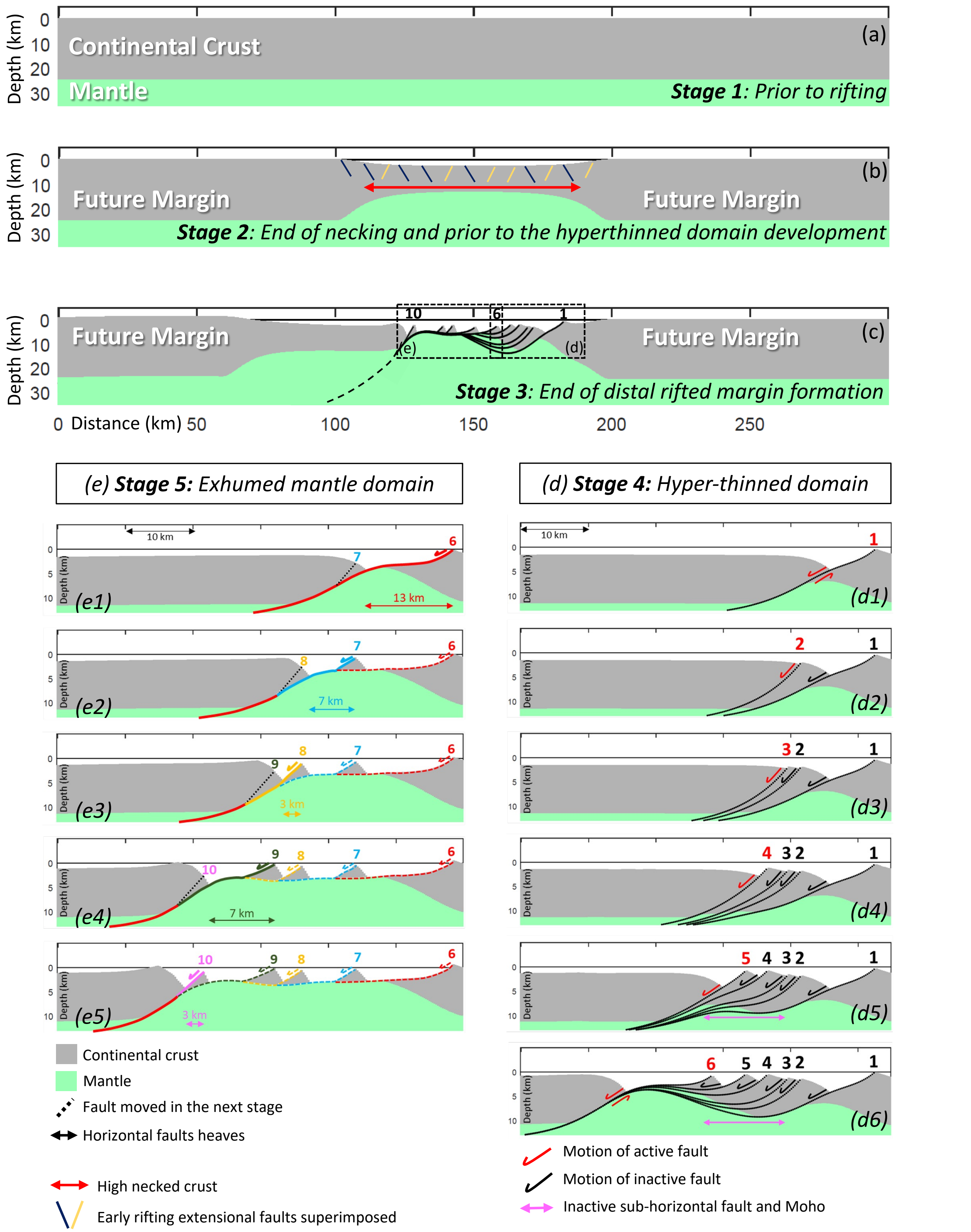

Figure 3: A generalized evolutionary RIFTER model showing the development of a magma-poor rifted margin. **a)** Lithosphere architecture prior to rifting. **b)** Lithosphere architecture at the end of the necking stage, prior to the formation of hyper-extended domain. **c)** Formation of hyper-thinned domain by in-sequence oceanward extensional faulting leading to mantle exhumation. **d)** Detail of the hyper-thinned domain formation (d1-d6). **e)** Detail of the exhumed mantle domain formation (e1-e5).

https://doi.org/10.5194/egusphere-2023-2171
Preprint. Discussion started: 28 September 2023

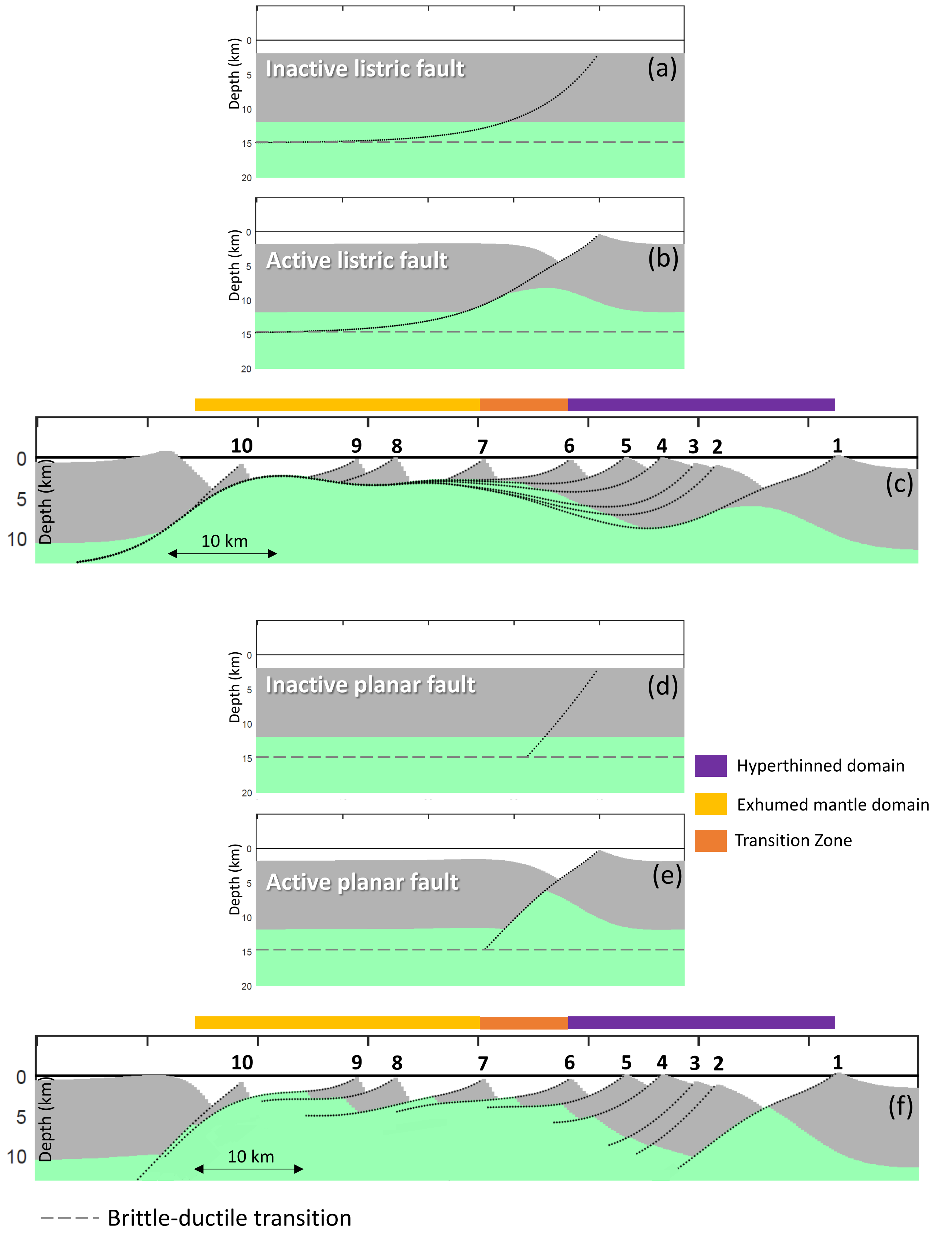

Figure 4: Comparison of hyper-extended domain structure and transition to exhumed mantle predicted using listric and planar faults in the RIFTER model. a-c) Using listric faults (same as shown in Figure 3c) and d-f) using planar faults.

https://doi.org/10.5194/egusphere-2023-2171
Preprint. Discussion started: 28 September 2023

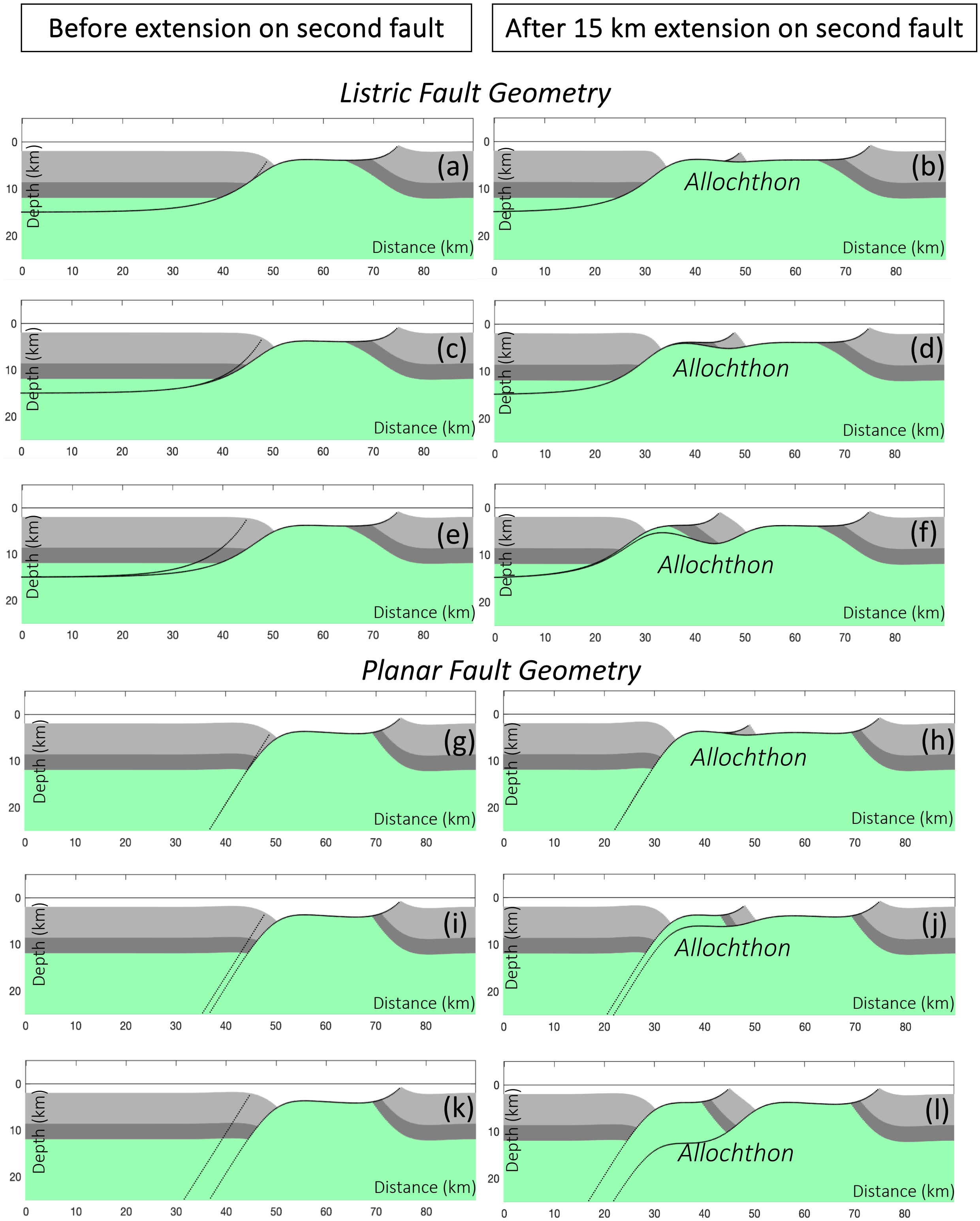

Figure 5: Comparison of allochthon block formation using listric (a-f) and planar (g-l) fault geometry for different offsets of new short-cut fault with respect to footwall emergence of primary fault. Initial fault dip 60°, detachment depth = 15 km for listric fault, Te = 0.5 km. a, b, g & h) 1 km offset of new short-cut fault with respect to footwall emergence of primary fault before and after 15 km of extension and predicted extensional allochthon block for listric and planar fault geometry. c, d, i & j) corresponding model prediction with 2 km offset. e, f, k & l) corresponding model prediction with 5 km offset.

https://doi.org/10.5194/egusphere-2023-2171
Preprint. Discussion started: 28 September 2023

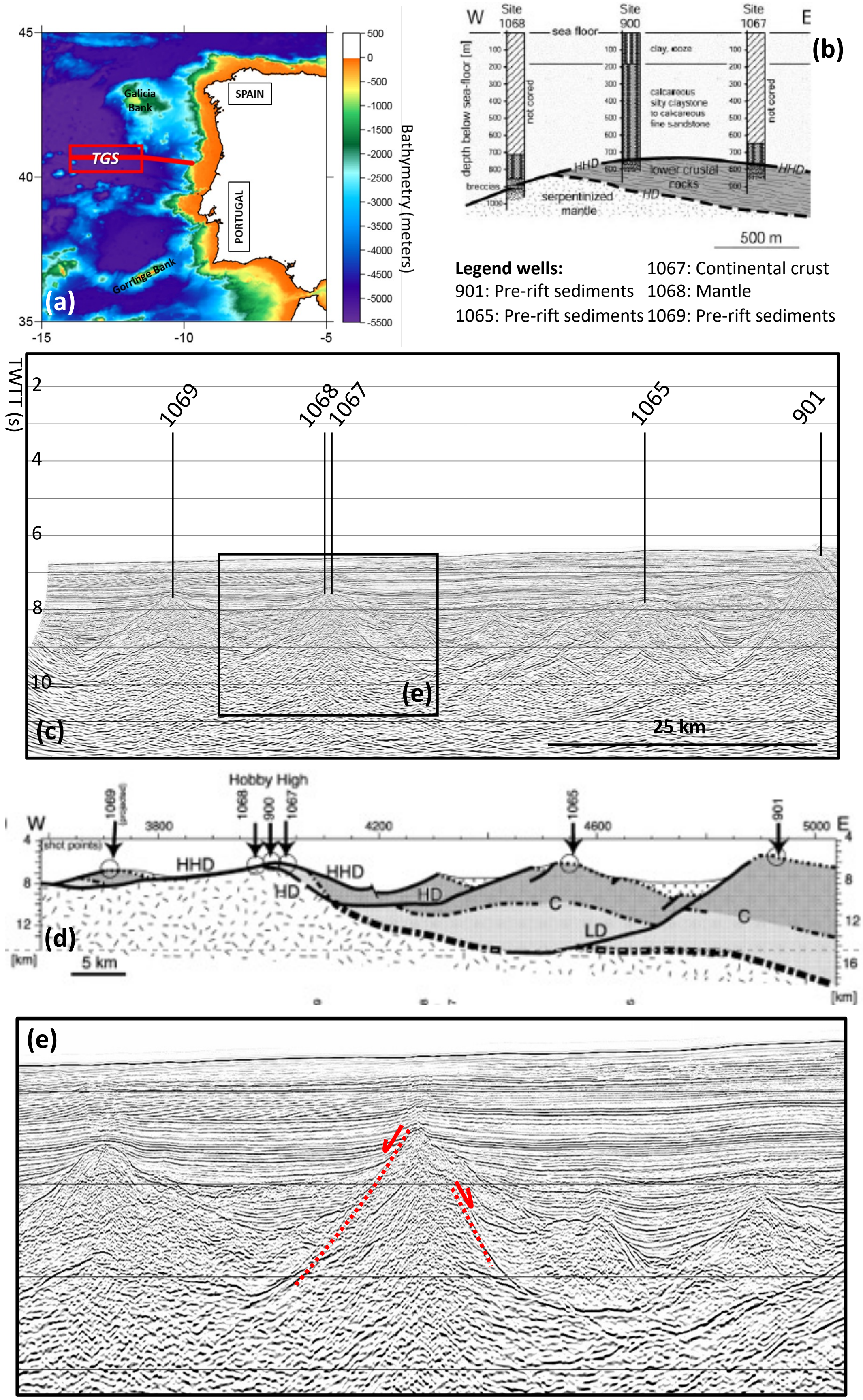

Figure 6: a) Bathymetric map of the western Iberian margin showing in red the location of TGS seismic reflection profile. b) ODP well observations from the western Iberia margin (Manatschal et al., 2001 and 2004). c) Part of the TGS time domain seismic reflection section (Sutra and Manatschal et al., 2012) showing ODP well locations (black lines). d) Interpretation of the above by Manatschal et al., (2001 and 2004). e) Interpretation of out-of-sequence faulting for inset of seismic section shown in c).

https://doi.org/10.5194/egusphere-2023-2171
Preprint. Discussion started: 28 September 2023

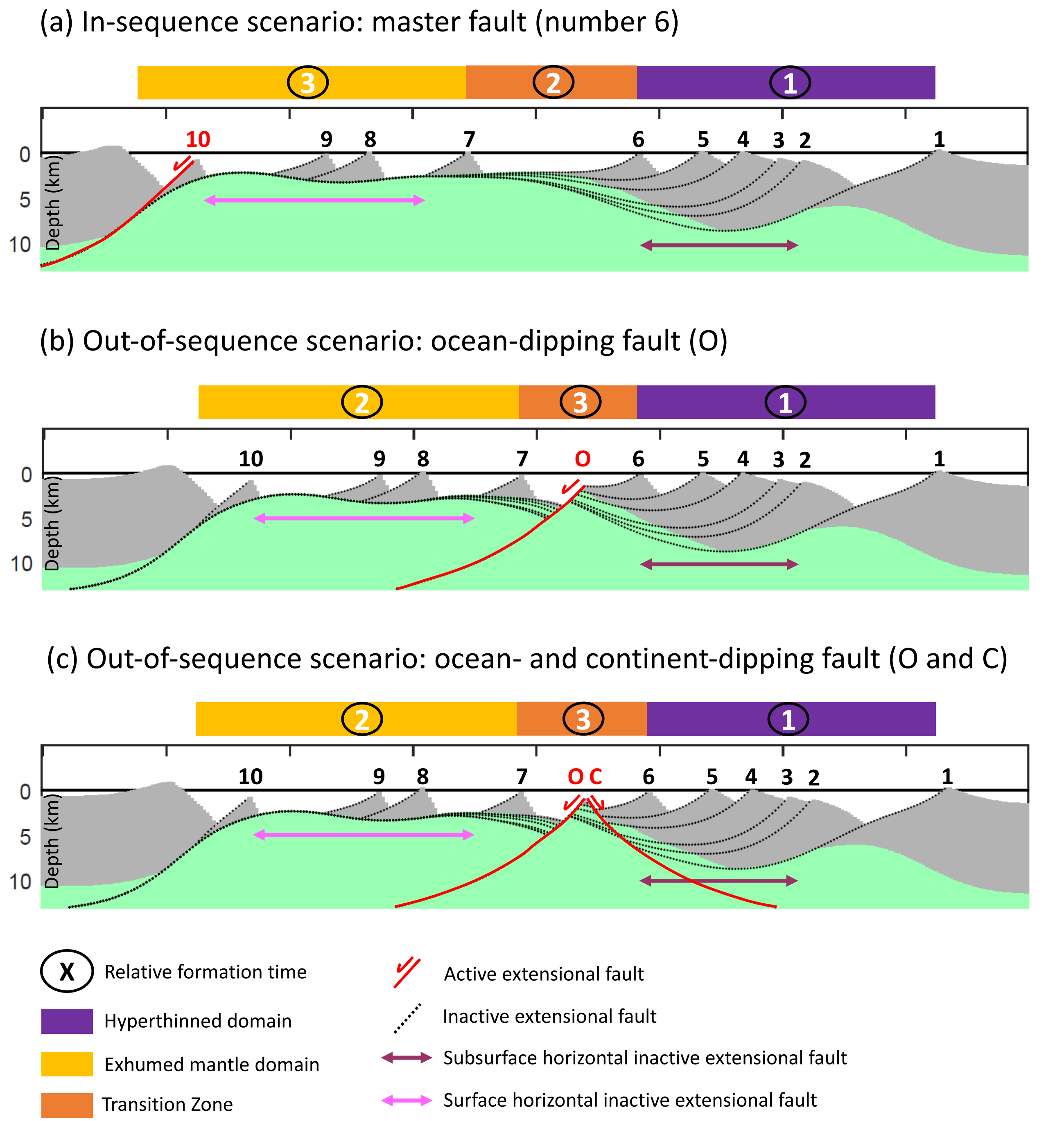

Figure 7: Comparison of predicted transition from hyper-extended crust onto exhumed mantle for in-sequence and out of sequence faulting. Crust and mantle are grey and green respectively. a) In-sequence faulting produces a smooth bathymetric transition from hyper-extended crust to exhumed mantle. b & c) Out of sequence faulting produces a transition from hyper-extended crust to exhumed mantle with bathymetric relief.

https://doi.org/10.5194/egusphere-2023-2171
Preprint. Discussion started: 28 September 2023

Faults numbers	1	2	3	4	5	6
Horizontal faults heaves (km)	7	0,5	0,5	1,5	4	13
Initial fault dip (listric fault)	Surface = 60°					
	At 15 km = 0°					
Fault movement	Red number = fault active					
	Black number = fault inactive					

Table 1: Table for fault parameters used for Figure 3d. Fault number indicates the chronological movement (Fault 1 is the oldest).

Faults numbers	6 (master fault)	7	8	9	10
Horizontal faults heaves (km)	13	7	3	7	3
Initial fault dip (listric fault)	Surface = 60°				
	At 15 km = 0°	At 30 km = 0°			
Fault movement	Colour solid line = fault active				
	Colour dash line = fault inactive				

Table 2: Table for fault parameters used in Figure 3e. Fault number indicates the chronological movement (Fault 6 is the oldest).

https://doi.org/10.5194/egusphere-2023-2171
Preprint. Discussion started: 28 September 2023

Domains formed	1. Hyperthinned domain		2. Transition zone	3. Exhumed mantle domain
Horizontal faults heaves (km)	Faults numbers	6 (master fault)		
	Horizontal faults heaves (km)	13		
	Initial fault dip (lisitric fault)	Surface = 60°		
		Depth at 15 km = 0°		

Table 3: Table for fault parameters used in Figure 7a.

Domains formed	1. Hyperthinned domain	2. Exhumed mantle domain	3. Transition zone
Horizontal faults heaves (km)	Faults numbers	6 (master fault)	Fault O (ocean)
	Horizontal faults heaves (km)	7	2
	Initial fault dip (lisitric fault)	Surface = 60°	Surface = 60°
		Depth at 15 km = 0°	Depth at 15 km = 0°

Table 4: Table for fault parameters used in Figure 7b.

Domains formed	1. Hyperthinned domain		2. Exhumed mantle domain	3. Transition zone
Horizontal faults heaves (km)	Faults numbers	6 (master fault)	Fault O (ocean)	Fault C (continent)
	Horizontal faults heaves (km)	7	2	1
	Initial fault dip (lisitric fault)	Surface = 60°	Surface = 60°	Surface = 60°
		Depth at 15 km = 0°	Depth at 15 km = 0°	Depth at 15 km = 0°

Table 5: Table for fault parameters used in Figure 7c.